Korean J Physiol Pharmacol
Vol 12: 323-330, December, 2008

Voltage-dependent Ca^{2+} Current Identified in Freshly Isolated Interstitial Cells of Cajal (ICC) of Guinea-pig Stomach

Young Chul Kim[1], Hikaru Suzuki[2], Wen-Xie Xu[3], Hikaru Hashitani[2], Woong Choi[4], Hyo-Yung Yun[5], Seon-Mee Park[6], Sei Jin Youn[6], Sang-Jeon Lee[5], and Sang Jin Lee[1]

[1]Department of Physiology, Chungbuk National University, College of Medicine, Cheongju 361-763, Korea, [2]Department of Physiology, Nagoya City University Medical School, Nagoya 467-8601, Japan, [3]Department of Physiology, College of Medicine, Shanghai Jiaotong University, Shanghai 200240, P.R. China, Departments of [4]Pharmacology, [5]Surgery, [6]Internal Medicine, Chungbuk National University, College of Medicine, Cheongju 361-763, Korea

The properties of voltage dependent Ca^{2+} current (VDCC) were investigated in interstitial cells of Cajal (ICC) distributed in the myenteric layer (ICC-MY) of guinea-pig antrum. In tissue, ICC-MY showed c-*Kit* positive reactions and produced driving potentials with the amplitude and frequency of about 62 mV and 2 times min^{-1}, respectively, in the presence of 1 μM nifedipine. Single ICC-MY isolated by enzyme treatment also showed c-*Kit* immunohistochemical reactivity. These cells were also identified by generation of spontaneous inward current under K^+-rich pipette solution. The voltage clamp experiments revealed the amplitude of - 329 pA inward current at irregular frequency. With Cs^+-rich pipette solution at V_h= - 80 mV, ICC-MY produced voltage-dependent inward currents (VDIC), and nifedipine (1 μM) blocked VDIC. Therefore, we successfully isolated c-*Kit* positive single ICC from guinea-pig stomach, and found that ICC-MY potently produced dihydropiridine sensitive L-type voltage-dependent Ca^{2+} currents ($VDCC_L$).

Key Words: Gastrointestinal (GI) tract, Stomach, Interstitial cells of Cajal (ICC), Voltage-dependent Ca^{2+} current (VDCC)

INTRODUCTION

Spontaneous activity of gastrointestinal (GI) smooth muscles originates from the interstitial cells of Cajal (ICC) in GI tract (Sanders, 1996). ICC express the proto-oncogene c-*Kit*, a receptor tyrosine kinase, which play an essential role for the development of ICC via its activation by a ligand, stem cell factor or "*Steel*" factor. In stomach, there are two types of ICC distributed in the wall, ICC-MY distributed in the myenteric layer between two layers of smooth muscle and ICC-IM distributed within smooth muscle bundles: ICC-MY produce a driving potential to promote smooth muscle contraction (Dickens et al, 1999), while ICC-IM produce a unitary potential with irregular transient depolarization and they are considered to take a role for the mediation of signal transduction between autonomic nerves and smooth muscle cells (Wang et al, 2003). Each of individual ICC has connection with neighboring ICC and also with smooth muscle cells through gap junctions, and therefore the changes in membrane potential occurred in individual ICC could be propagated to a wide range of gastric wall (Hirst & Ward, 2003). Because of these reasons, it is known that ICC plays important roles in regulation of GI motility. In accordance with this conception, significant change such as constructional destruction, acquired megacolon and infantile hypertrophic pyloric stenosis has been implicated in many GI disorders (Kubota et al, 2005; Lee et al, 2005; Oue & Puri, 1999).

ICC-MY distributed in the antrum of stomach produce driving potential which has initial fast rising, followed by plateau phases. The plateau phase may be produced by an activation of Ca^{2+} activated Cl^- currents, while the initial phase may be produced by voltage-dependent Ca^{2+} currents (VDCCs) (Hirst & Edward, 2001; Kito & Suzuki, 2003). Since the component of the plateau phase is sensitive to dysfunction of internal Ca^{2+} store (sarcoplasmic reticulum, SR) with cyclopiazonic acid (CPA) (Kito & Suzuki, 2003), Ca^{2+} released from SR may play an important role in the regulation.

Several types of ion channels have been suggested to play a role in the generation of driving potential in GI tissues, and Ca^{2+}-inhibited nonselective cationic and Ca^{2+}-activated Cl^- channels have been suggested as the major pathway for producing pacemaker potential in ICC-MY of the murine small intestine (Thomsen et al, 1998; Hirst & Ward, 2003). VDCC has also been suggested as a main contributor to

Corresponding to: Young Chul Kim, Department of Physiology Chungbuk National University College of Medicine, 12, Gaeshin-dong, Heungduk-gu, Cheongju 361-763, Korea. (Tel) 82-43-261- 2859, (Fax) 82-43-261-2859, (E-mail) physiokyc@chungbuk.ac.kr

ABBREVIATIONS: VDCC, voltage-dependent Ca^{2+} current; ICC, interstitial cells of Cajal; ICC-MY, ICC from myenteric border; VDIC, voltage-dependent inward current; $VDCC_L$, L-type voltage-dependent Ca^{2+} current; GI tract, gastrointestinal tract; ICC-IM, ICC distributed within smooth muscle bundle; SR, sarcoplasmic reticulum; CPA, cyclopiazonic acid; PSS, physiological salt solution; EGTA, ethyleneglycol bis-(β-aminoethylether)-*N,N,N',N'*-tetraacetic acid.

the formation and regulation of pacemaker potential in ICC of the small intestine (Koh et al, 1998; Thomsen et al, 1998; Koh et al, 2002; Ward et al, 2004). In addition to these main channels, Kim (Kim et al, 2002) also reported the expression of two types of VDCCs in cultured ICC which were prepared from the murine intestine and colon (Langton et al, 1989; Ward & Sanders, 1992; Lee & Sanders, 1993; Kim et al, 2002). It is generally reasonable to suggest that the dihydropyridine-insensitive VDCC participates in the upstroke component of pacemaker potential (Ward & Sanders, 1992; Kim et al, 2002; Kito et al, 2005). However, recent reports suggest that in mouse and human ICC do not express VDCC (Ördög et al, 2004).

In the present study, we examined the distribution of VDCC in ICC-MY of the antrum of stomach. Thus, we prepared a single ICC-MY from the antrum, and the patch clamp technique was applied to analysis of VDCC.

METHODS

Preparation of ICC

Guinea-pigs, weighing 300~350 g, were anesthetized with fluoromethyl 2,2,2-trifluoro-1(trifluoromethyl) ethyl ether (sevoflurane, Maruishi Pharma., Osaka, Japan), and exsanguinated after stunning or decapitation. All experiments were performed in accordance with the guidelines for the animal care and use approved by the Chungbuk National University, The Physiological Society of Japan and Shanghai Jiaotong University, respectively. The antral portion of stomach was cut, and the mucosal layer was separated from the muscle layers in Ca^{2+}-free physiological salt solution (Ca^{2+}-free PSS). Circular muscle layer of the tissues was carefully removed from the longitudinal layer by sharp dissection with fine scissors under a dissecting microscopy. This circular free tissue was cut into small segments (3×3 mm). These segments were incubated in Ca^{2+}-free PSS for an hour at 4°C. Then, they were incubated for 10~15 min at 36°C in the Ca^{2+}-free PSS containing 0.1 % collagenase (Wako, Osaka, Japan), 0.05 % dithiothreitol, 0.1% trypsin inhibitor and 0.2 % bovine serum albumin. After the digestion, the supernatant was discarded, and the softened muscle segments were transferred into Ca^{2+}-free PSS, and single cells were then dispersed by gentle agitation with a wide-bore glass pipette. Single ICC was isolated by using this process and isolated gastric ICC was kept in Ca^{2+}-free PSS at 4°C until use. All the experiments were carried out within 8 hours after harvesting cells. Temperature of experiments was constantly controlled at 36°C for conventional sharp electrode recording, 32°C for conventional whole-cell voltage clamp.

Tissue preparation for sharp electrode recording

The excised stomach was opened by cutting along the small curvature in Krebs solution. The mucosal layer was removed by cutting with fine scissors, and smooth muscle tissues were isolated from the antral region. Under a dissecting microscopy, the circular muscle layer was carefully removed and a segment (about 1.5 mm wide and 3 mm long) of longitudinal smooth muscle layer, with attached myenteric border, was prepared. The tissue was pinned out on a silicon rubber plate fixed at the bottom of the organ bath (8 mm wide, 8 mm deep, 20 mm long), with the myenteric border uppermost. The tissue was superfused with warmed (36°C) and oxygenated Krebs solution, at a constant flow rate of about 2 ml/min. Experiments were carried out in the presence of 1 μM nifedipine, so as to minimize muscle movements. However, some experiments were carried out in the absence of nifedipine.

Conventional microelectrode technique was used to record intracellular electrical responses of ICC-MY or smooth muscle cells. Briefly, glass capillary microelectrodes (outer diameter, 1.2 mm, inner diameter 0.6 mm; Hilgenberg, Germany) filled with 0.5 M KCl, with the tip resistances ranging between 50~80 MΩ, were inserted to cells. Electrical responses recorded were amplified through a high input impedance amplifier (Axoclamp-2B, Axon Instruments, Foster City, Calif., USA), and were also displayed on a cathode-ray oscilloscope (SS-7602, Iwatsu, Osaka, Japan). The responses were also stored on a personal computer for later analysis of the data.

Voltage-clamp patch experiments

Isolated cells were transferred to a small chamber on the stage of an inverted microscopy (IX-70 or IX-71, Olympus, Japan). The chamber was perfused with PSS (2~3 ml/min). Glass pipettes with a resistance of 2~5 MΩ were used to make a giga seal of 5~10 GΩ, by using standard patch clamp techniques (Hamil et al, 1981). Membrane currents were amplified with an axopatch-1C, 200B patch-clamp amplifier (Axon Instruments, Calif., USA), and data were digitized with Digidata 1220 or Digidata 1322 and stored directly and digitized on-line using pClamp software (version 5.5.1 or 9.2). Data were displayed on a digital oscilloscope, pen recorder (Gould, Cleveland, Ohio, USA) and a computer monitor, and data were analyzed using pClamp 6.0 (pClamp 9.2) and Origin software 6.1.

Solution and drugs

The Ca^{2+} PSS contained the following composition (in mM): NaCl 140, KCl 4.5, $CaCl_2$ 2, $MgCl_2$ 1, glucose 10, and HEPES (N-[2-hydroxyethyl] piperazine-N'-[2-ethanesulphonic acid]) 10, and its pH was adjusted to 7.4 with NaOH. Phosphate-added cold Tyrode's solution containing (mM): NaCl 145, KCl 5, $MgCl_2$ 2, $CaCl_2$ 2, glucose 10, NaH_2PO_4 0.42, Na_2HPO_4 1.81, HEPES 10, pH 7.4. KRB solution (CO_2/bicarbonate-buffered Tyrode) contained (in mM) NaCl 122, KCl 4.7, $MgCl_2$ 1, $CaCl_2$ 2, $NaHCO_3$ 15, KH_2PO_4 0.93, and glucose 11 (pH 7.3~7.4, bubbled with 5 % CO_2/95 % O_2). For recording of the pacemaker currents, the pipette solution contained (mM): KCl 140, $MgCl_2$ 5, K_2ATP 2.7, Na_2GTP 0.1, creatine phosphate 2.5 (disodium salt), HEPES 5 and EGTA 0.1, and pH was adjusted to 7.2 by Tris (this is referred to as the K^+-rich pipette solution in the text). The Cs^+-rich pipette solution for the recording of pacemaker and voltage- dependent inward currents contained: 120 CsCl, 20 TEACl, 0.1 ethyleneglycol bis-(β- aminoethyl ether- *N,N,N',N'*-tetraacetic acid (EGTA), 10 HEPES, 4 MgATP, 1 Na_2GTP, 2 creatine phosphate (disodium salt) and pH was adjusted to 7.2 by Tris. All drugs used in this study were purchased from Sigma.

Immunohistochemical labeling of ICC

The stomach was cut along the lower curvature and the mucosa and circular muscle layers dissected away. For the

detection of c-*Kit* positive ICC-IM, the longitudinal muscle layer was carefully removed by fine scissors. Preparations were processed immunohistochemically to reveal ICC using an antibody. To visualize cells expressing c-*Kit* immunoreactivity, tissues and single isolated ICC was incubated for an hour in PSS containing monoclonal antibodies raised against the c-*Kit* protein (ACK-2, diluted 1 : 100, eBioscience, USA) (Kim et al, 2002). The tissue was washed 5 times with physiological saline, and single ICC was centrifused (800 rpm, 2 min) and the suspension was washed for 4 times with PSS. Then, tissue and single isolated ICC was incubated for additional 1 hour in an anti-rat IgG antibody labeled with a fluorescent marker (goat anti-rat IgG Texas Red, 1 : 500, Molecular probes, USA). Patch clamp study was done using ICC which showed c-*Kit* activity. The tissue preparation was then pinned out on a Sylgard block (silicone elastomer, Dow Corning Corporation, U.S.A) which had window of some 3×3 mm in the center. The Sylgard block was turned over and then placed at the bottom of the chamber, so that the preparation faced a glass coverslip. The distribution of ICC-MY was determined by constructing z-stacks from the myenteric region where networks of c-*Kit* positive cell were apparent in guinea-pig stomach. The distribution of ICC-IM was determined by optically sectioning through the circular layer. The cells were examined with a Leica Type TCS SP2 AOBS confocal microscope (Leica Microsystems, Heidelberg GmbH, Germany) with a Leica inverted microscope (Leica DMIRE2, Leica, Germany). A 40.0×(NA 0.75) dry objentive lens was used (Leica Microsystems, Germany). Confocal images were captured with an excitation wave length appropriate for Texas Red (488 nm). Final images were constructed with Leica Confocal Software Ver. 3.0 (Leica Microsystem).

Statistics

Data were expressed as means±standard errors of the mean (means±SEM). Experimental number (n) of result represents number of tested cells and tissues during experiments. The Student's *t*-test was used wherever appropriate, to evaluate the differences in data. P values less than 0.05 were considered statistically significant.

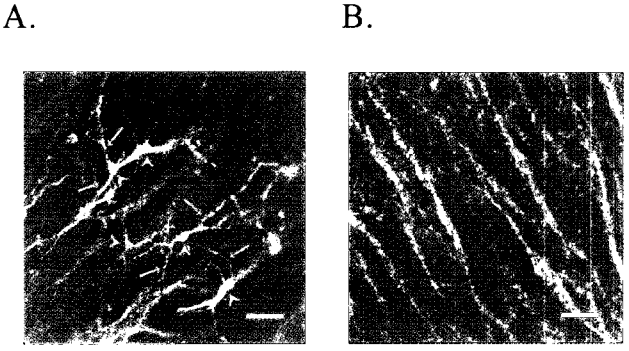

Fig. 1. Identification of ICC in the antral region of guinea-pig stomach by c-*Kit* immunohistochemical activity. (A) reveals the network of ICC-MY in myenteric border of guinea-pig gastric antrum. In (A), arrow head and arrow indicate cell body and processes from ICC-MY, respectively. (B) ICC-IM in circular muscle layers is shown. Scale bars in (A) and (B) are 40 μM.

RESULTS

Distributions of ICC-MY in gastric antrum of guinea-pig stomach

Under confocal microscopy, c-*Kit* immunoreactivity was detected in the myenteric border. As shown in Fig. 1A, the observed cells showed multiple processes from the cell body, and these cells were connected to each other to form two dimensional networks in myenteric border (n=5). These phenotypes and c-*Kit* reactivity represent ICC-MY (Komuro et al, 1996). In Fig. 1B, c-*Kit* positive ICC-IM was also identified in circular muscle bundle through optically sectioning (n=5).

Spontaneous electrical activity from ICC-MY of guinea-pig stomach

Driving potentials (plateau-type potentials with fast rate of rise) from ICC-MY were recorded from myenteric border of guinea-pig antrum (Fig. 2). Their features of fast upstroke, peak amplitude and plateau state in 11 different tissues are shown in Fig. 2. The frequency of driving potentials was 2.3±0.4 times/min, and their mean amplitude and maximum rate of rise (dV/dt_{max}) were 62±1.7 mV and 1,031±79 mV/sec, respectively (n=11). Resting membrane potential was −68.5±3.5 mV (n=11).

Identification of single ICC-MY

As shown in Fig. 3A and 3B, ICC-MY from myenteric border had many processes (Fig. 3A and 3B) and it was absolutely discernable, compared to spindle like and non branched smooth muscle cell (data not shown). Fresh single ICC expressed c-*Kit* immunoreactivity under confocal mi-

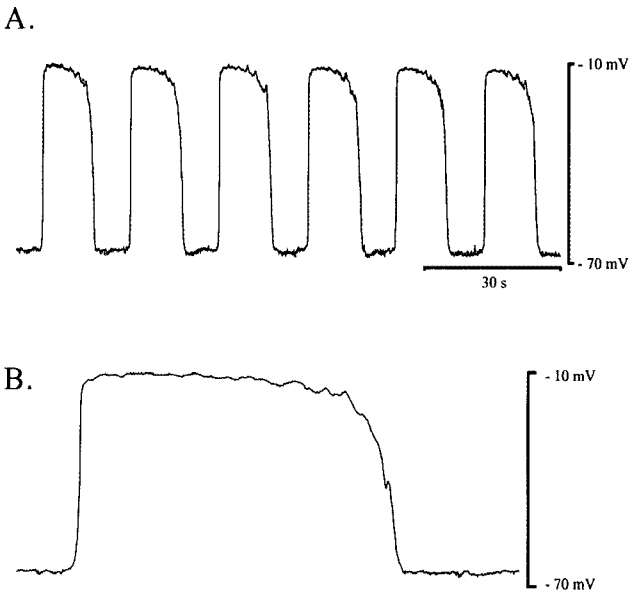

Fig. 2. Pacemaker potential of ICC-MY in myenteric area of guinea-pig gastric antrum. Spontaneous electrical activity of ICC-MY in guinea-pig antrum was recorded in the presence of 1 μM nifedipine. (A) and (B) Driving potential from ICC-MY was recorded in the presence of 1 μM nifedipine. (B) Expended event of pacemaker potential was displayed.

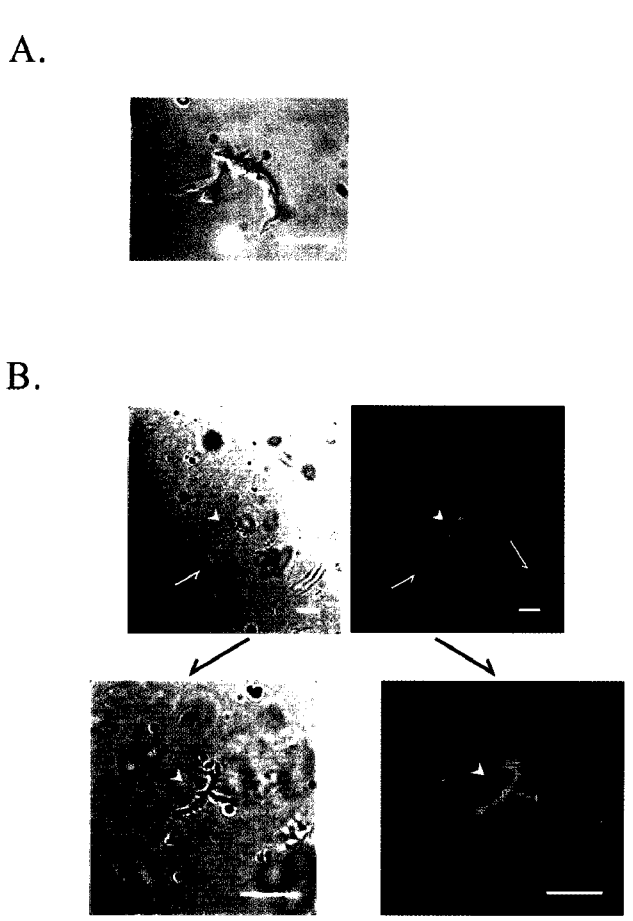

Fig. 3. Identification of freshly isolated single ICC-MY. Single ICC was isolated by enzyme treatment from myenteric border of gastric antrum in guinea-pig. (A) ICC-MY with many processes from myenteric border of guinea-pig gastric antrum is shown. ICC expressed c-*Kit* activity (B). (B) shows phenotype (left; arrow head) and c-*Kit* immunohistochemical reactivity (right; arrow head) of ICC-MY. Lower figures of (B) represent magnification of the upper (B). However, gastric smooth muscle cells (arrows) did not express c-*Kit* activity (right upper panel). Scale bars in (A) and (B) indicate 40 μM. Note: The left side of panel (B) is phase contrast image from guinea-pig gastric ICC. The right side of panel (B) is c-*Kit* immunoreactivity image.

croscopy (Fig. 3B). The cells isolated from guinea-pig antral myenteric border showed typical ICC phenotype and c-*Kit* immunohistochemical reactivity. For further confirmation, attempts were also made to record spontaneous current from ICC. Under conventional whole-cell voltage clamp and K^+-rich pipette solution (V_h=−90 mV), freshly isolated ICC generated spontaneous inward current with mean amplitude of −329±107.2 pA (n=14; Fig. 4A).

Characterization of voltage-dependent inward currents (VDIC) in single ICC-MY

Voltage clamp experiments were performed to characterize VDCC in freshly isolated single ICC from guinea-pig antrum. VDCC was recorded under conventional whole-cell configuration at 32°C, before and after the addition of 1 μM nifedipine. The Cs^+-rich pipette solution (see Methods for details) used to block outward currents and 2 mM Ca^{2+} was bathed outside as a charge carrier to record VDCC.

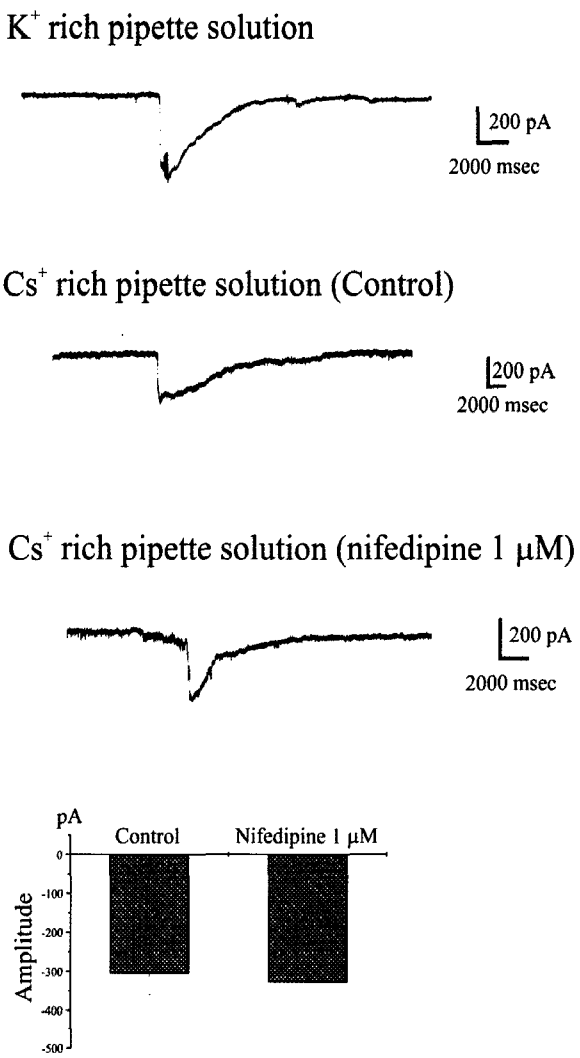

Fig. 4. Spontaneous inward current recorded from freshly isolated single gastric ICC from guinea-pig antrum. Using the conventional whole cell patch-clamp technique, we observed spontaneous inward current in freshly isolated single ICC from guinea-pig gastric antrum. (A) Spontaneous inward current was recorded irregularly under K^+-rich pipette solution. (B) and (C) ICC showed spontaneous inward current in the presence (C) and absence (B) of 1 μM nifedipine under Cs^+-rich pipette solution. The data from (B) and (C) are summarized in (D).

Before recording VDCC, spontaneous inward current was recorded to identify ICC at holding potential of −80 mV as shown in Fig. 4B. The spontaneous currents in the presence and absence of nifedipine were −329±101.7 pA (n=7) and −305±54.7 pA (n=15) in amplitude, respectively (Fig. 4B, 4C and 4D). The cells were stepped for 450 msec every 10 s from −80 to +40 mV by 20 mV increments from V_h of −80 mV. As seen in Fig. 5A and 5B, depolarization induced transient VDIC that consisted of a rapid activation phase, followed by partial inactivation. Near 0 mV, peak currents were observed, and the currents were reversed at +31±2.5 mV (n=6, Fig. 5C). Nifedipine blocked the peak current of VDICs (Fig. 5B~D). In the absence and presence of nifedipine, the amplitude of the peak inward current was −113±14.5 pA and −9±2.2 pA, respectively (n=5, $P<0.05$, Fig. 5D).

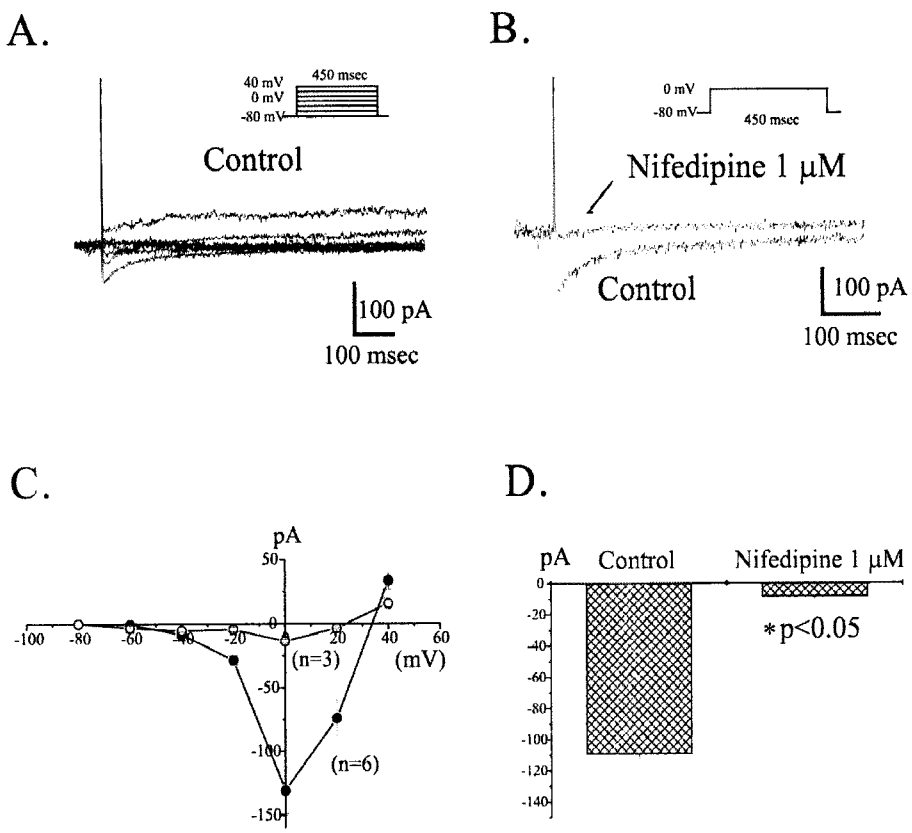

Fig. 5. Voltage-dependent Ca^{2+} currents (VDCC) in freshly isolated single ICC from guinea-pig antrum. At a holding potential of -80 mV, spontaneous inward current was recorded in freshly isolated single ICC as shown in Fig. 4B. From these cells, voltage-dependent inward current (VDIC) was recorded by step pulses. (A) Currents were elicited by 20 mV depolarizing step pulses from a holding potential of −80 mV to +40 mV (voltage protocol is shown in inset). (B) Currents were elicited by voltage steps from a holding potential of −80 mV to 0 mV. The peak amplitudes generated were compared before and after nifedipine (1 μM) treatment. (C) Current-voltage relationships of before (filled circles) and after (open circles) treatment of 1 μM nifedipine are shown. (D) The blocking effect of nifedipine on VDIC is summarized.

Steady state activation and inactivation kinetics of VDIC in single ICC-MY

The steady-state activation and inactivation properties of the VDIC were studied. To evaluate steady-state activation relationships, the peak conductance at each test potential was calculated using the equation: $I_{Ca} = g_{Ca} \times (V - E_{rev})$ where g_{Ca}, V, and E_{rev} were peak conductance, test potential and reversal potential, respectively. When the results were plotted, they fitted well with a Boltzmann equation. The half-activation voltage of VDIC before the application of nifedipine was of −1±2.9 mV (n=8) with a slope factor (k) of 8±1.6 (n=8; Fig. 6B).

A modified double-pulse protocol was used to measure steady-state inactivation of the VDIC as a function of membrane potential. Conditioning steps from −120 to +20 mV were applied for 3.75 sec. After a 7 msec step to −60 mV, the membrane potential was stepped to 0 mV for 1 sec. In Fig 6A and 6B, representative raw traces during applying inactivation protocol to cells in the presence and absence of 1 μM nifedipine are shown. Note that there were spontaneous inward currents generated in ICC during the recording (see arrows in Figure 6A and 6B). Resulting currents were normalized to the maximum current obtained after a conditioning potential of −120 mV (I/I_{max}) and plotted as a function of the conditioning potential. The data fitted well to a Boltzmann equation. Freshly isolated single ICC from guinea-pig gastric antrum had a half-inactivation voltage ($V_{0.5}$) of −48±11 mV with slope factor (k) 9±1.2 (n=4; Fig. 6B).

DISCUSSION

In the present study, we established a method for isolating and identifying single ICC-MY from guinea-pig antrum after enzymatic dispersion. Isolated single ICC-MY expressed $VDCC_L$ which was sensitive to nifedipine. Therefore, this study is expected to be useful for elucidating mechanism of gastric rhythmicity in human ICC.

Until now single ICC of GI tract was obtained by extracting cells from new born mice (10~13 days after birth) and then culturing them. However, this process clearly has limitations in its application to human. Therefore, we developed a new method to isolate single ICC directly from stomach of adult animal (Fig. 3A, B). The cells under phase contrast microscopy showed multiple processes and were distinguished from spindle like smooth muscle cells, and they expressed c-*Kit* reactivity (Fig. 3A, B). In contrast, smooth muscle cells did not express c-*Kit* activity (arrows in Fig. 3B). For further confirmation of identity of ICC, the patch clamp technique was employed as shown in Fig. 4A. Freshly isolated ICC-MY generated spontaneous current, however, it was still irregular. Unfortunately, we could not explain the reason of why spontaneous response of a single cell is so sparse compared to that from intact tissue or cell networks. Synergistic action among individual cells might be a plausible explanation for the strong and regular pacemaker potential in tissue.

Recently, Goto et al. (2004) and Wang et al. (2008) also suggested new method to isolate ICC from small intestine. Unfortunately, however, these techniques may not exclude possible connection of cells in network. As a criterion to identify ICC, molecular study might be one of powerful

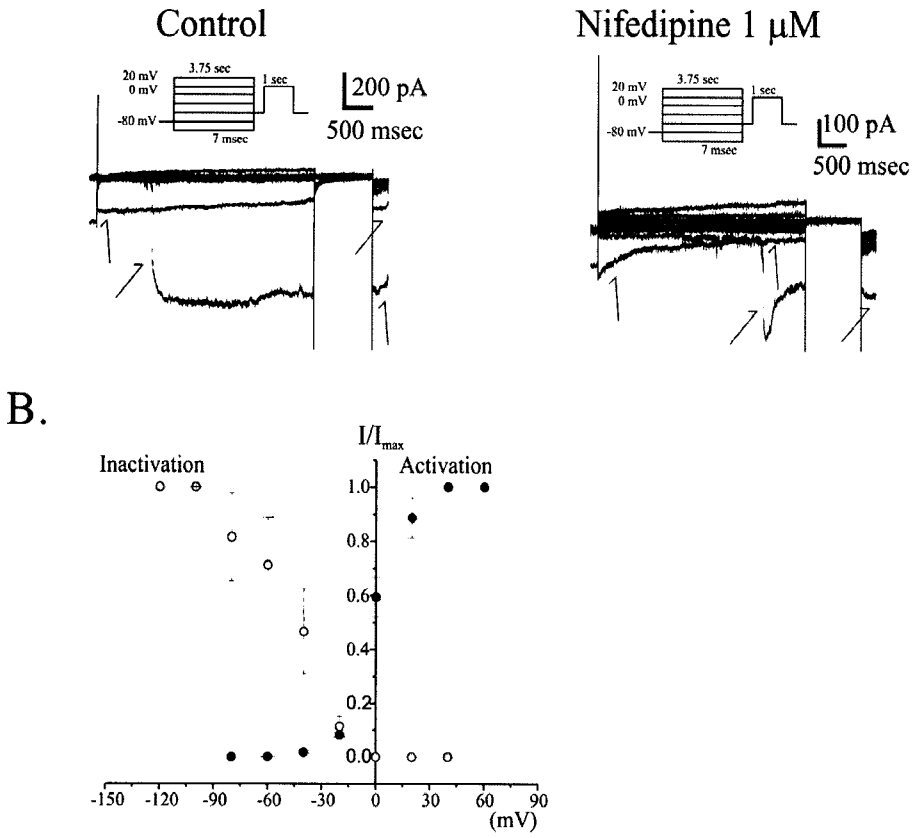

Fig. 6. Voltage-dependent activation and inactivation kinetics of VDIC in freshly isolated single ICC from guinea-pig antrum. Voltage dependences of activation and inactivation curves of VDIC are shown as a plot of normalized peak currents. (A) Raw current traces recorded for the analysis of steady-state inactivation before (left pannel) and after (right pannel) treatment of 1 μM nifedipine are shown. Note that generation of spontaneous inward current during the recording of VDCC (see arrows in (A)). (B) The steady-state activation and inactivation curves in the absence of nifedipine are plotted and displayed. Filled circles and open circles represent the activation and the inactivation curve, respectively. In the absence of nifedipine, a half-activation and -inactivation voltage ($V_{0.5}$) were -1 ± 2.9 mV and -48 ± 11 mV, respectively. And slope factors (k) of them were 8±1.6 and 9±1.2, respectively.

methods. In fact, ICC expresses the receptor tyrosine kinase, *Kit* (Ward et al, 1994; Huizinga et al, 1995; Torihashi et al, 1995;) and depend on the *Kit* signaling pathway for development and maintenance of their morphology (Torihashi et al, 1995; Torihashi et al, 1997; Klüppel et al, 1998; Beckett et al, 2007). Through single-cell RT-PCR studies, ICC from small intestine was also identified by detection of 258 bp *Kit* mRNA in agarose gel electrophoresis (Thomsen et al, 1998). In our study, we identified ICC by their immunohistochemical identity in addition to electrical and morphological identities. We are also in a process to study further in future.

As shown in Fig. 2, we recorded pacemaker potentials and c-*Kit* immunoreactivity in ICC-MY from guinea-pig (Fig. 1A). Even though we isolated ICC-MY (Fig. 3B~D), it is difficult to be certain whether we selectively isolated only ICC-MY, since there are at least two types of ICC in GI tract. However, it was also suggested that ICC-MY and ICC-IM (or ICC-DMP) have somewhat different characteristics (see introduction) (Ördög T, 2004). In that study, it was reported that murine and human ICC-DMP/IM did not express L- and T-type Ca^{2+} channels but they only expressed several types of neurotransmitter receptors such as muscarinic receptors (Ördög T, 2004). Therefore, at the moment, the existence of VDCC was denied in ICC-IM. In addition, we recorded VDCC in electrically spontaneous and rhythmical ICC as shown in Fig. 4 and Fig. 6A. Since ICC-MY is known to produce a driving potential to promote smooth muscle contraction via gap junction [Dickens et al, 1999], we believed that we could record VDCC from ICC-MY. In fact, VDCCs were isolated from cultured ICC of intestine and colon (Kim et al, 2002), and dihydropyridine insensitive VDCC was suggested to possibly be a necessary component of slow wave propagation and/or upstroke potential (Ward et al, 1992; Kim et al, 2002; Hennig et al, 2004). In GI tract, several types of VDICs were reported (Langton et al, 1989; Ward et al, 1992; Koh et al, 2001; Kim et al, 2002) and their characteristics were compared (Kim et al, 2002). As shown in Fig. 4B~D, we recorded spontaneous inward current under Cs^+ rich pipette solution in freshly isolated ICC from guinea-pig antrum. Under this condition, spontaneous inward currents were recorded with amplitude of -329 ± 101.7 pA and -305 ± 54.7 pA in the presence and absence of nifedipine, respectively (Fig. 4B, C and 4D). Spontaneous inward current was recorded at V_h of -80 mV since the same V_h was applied to cells for recording of VDCCs in the same condition. From these cells, we recorded VDIC which is significantly inhibited by nifedipine (Fig. 5B~D), implying over 90% of the currents are $VDCC_L$. However, the data need to be carefully interpretated since the remaining current was too small and rundown of VDCC should be considered. In contrast, about 50% of the VDCC in murine small intestine and colon are L-type, since it is reduced to 50% of the control by nicardipine, and half of the remaining portion was mibefradil sensitive non-L-type current (IC_{50}=73 nM) (Kim et al, 2002). Even though ICC was first identified in GI tract, the existence of ICC other smooth muscle organ were

also reported (Sergeant et al, 2000; Pucovsky et al, 2003). In freshly isolated ICC from mesenteric artery and urethra, $VDCC_L$ which is blocked by 10 μM nicardipine or nifedipine was recorded. Therefore, $VDCC_L$ in freshly isolated ICC including ICC from guinea-pig stomach is believed to more prominent (Sergeant et al, 2000; Pucovsky et al, 2003).

Dihydropyridine insensitive VDCC has already been reported to be involved in the regulation of propagation and/or upstroke potential of slow wave (Ward & Sanders, 1992; Kim et al, 2002; Hennig et al, 2004; Ward et al, 2004), and we also tried to elucidate possible involvement of $VDCC_L$ in spontaneous rhythmicity (data not shown). To date, $VDCC_L$ has not been regarded as a contributor to the regulation of rhythmicity in ICC. Furthermore, it is nearly impossible to record rhythmicity without dihydropiridine, therefore, driving potentials were recorded always after application of nifedipine (Fig. 2). In this study, we tried to record driving potentials without nifedipine, however, we obtained only two successful recordings, and only one of them was suitable for the analysis (data not shown). In that recording, we found similar general features of driving potentials in both cases: The frequency, mean amplitude and dV/dt in the absence of nifedipine were 2.5 times min^{-1}, 54 mV and 951 mV/sec, respectively. And half- width of driving potential in the absence of nifedipine was 4.7 sec and the same value was 6.8±1.0 sec in the presence of nifedipine (n=3). However, the spike potentials were superimposed on the plateau, and became more prominent without nifedipine. In fact, dihydropiridine-resistant VDCC is known to be related to mechanism of entrainment of spontaneous rhythmicity (Ward et al, 2004). Therefore, $VDCC_L$ seems also to be related to the generation of spike potential on driving potential. Since spontaneous rhythmicity is dihydropyridine insensitive, $VDCC_L$ may be involved such as generation of spike potential in ICC and synergistic action among single ICC for regular spontaneous rhythmicity in network ICC and so on. It should be studied in the future.

As shown in Fig. 6B, we also studied kinetic characteristics of VDIC of single ICC. The single ICC had a half-activation voltage ($V_{0.5}$) of −1±2.9 mV with a slope factor (k) of 8±1.6 (Fig. 4B). After nifedipine treatment, the half-activation voltage of nifedipine-insentive current was shifted to the left (−7±2.4 mV, n=3; $p<0.05$), while the slope factor was decreased to 7±0.16 (data not shown). However, the activation kinetics was quite different compared to those from murine ICC and even guinea-pig gastric smooth muscle. In the case of murine colonic (small intestine) ICC, the values of $V_{0.5}$ were −12 mV (−15 mV) and −19 mV (−26 mV) in the presence and absence of nicardipine, respectively (Kim et al, 2002). In GI tract, stomach (4±0.2 cycle/min) and intestine (26±2.8 cycle/min) show different patterns of slow wave frequency and motility (Dickens et al, 2001; Kito et al, 2005), and different contribution of VDCC has been suggested as one of plausible mechanisms responsible for such differences (Malysz et al, 1995; Cayabyab et al, 1996). Therefore, each characteristics of ICC might be different, depending on the types of ICC and/or their origin. Especially, it is also known that the slow wave from stomach was not continuous but it was suddenly blocked at the level of pyloric sphincter (Lammers et al, 1998). It should particularly be noted that the slow wave from stomach is known to suddenly be blocked at pyloric sphincter where ICC-AP is absent (Wang et al, 2005). In our previous study, we also reported that $V_{0.5}$ in gastric smooth muscle was about −13 mV in the absence of dihydropyridine (Xu et al, 1996). Therefore, the value from gastric ICC might also be different from that of gastric smooth muscle. In fact, these values are different depending on the types of VDIC (Langton et al, 1989; Ward et al, 1992; Koh et al, 2001; Kim et al, 2002). However, since the activation voltage range is somewhat different between these cells, $VDCC_L$ of both cells in stomach might have different roles played in gastric motility, which needs to be studied in future.

And in the case of inactivation kinetics, average half-inactivation voltage was −48±11.9 mV with slope factor (k) 9±1.2 (Fig. 6B). However, inactivation curve was almost unavailable after nifedipine treatment since the currents were nearly abolished. In two cases where analyses were possible, the values of half-inactivation voltage was shifted left to −78 mV and the slope factor decreased to 4. Unfortunately, we had difficulties for the analysis of non-L type VDCC for above reasons. However, at this moment, we can give strong evidence of the expression of $VDCC_L$ in freshly isolated single ICC which shows spontaneous electrical activity in guinea-pig gastric antrum. This was done by isolating ICC-MY in myenteric border from antral region of stomach in adult animal by simple enzyme treatment. However, molecular and single channel study will be necessary to identify the existence of non-L type VDCC in freshly isolated ICC in the future.

In summary our results indicated that freshly isolated single ICC showed typical multi-processed morphology, c-*Kit* immunohistochemical activity. And it produced spontaneous inward current generation, and $VDCC_L$ in freshly isolated single ICC.

ACKNOWLEDGEMENT

This work was supported by Korea Research Foundation Grant (KRF-2004-205-E00001).

REFERENCE

Beckett EAH, Ro S, Bayquinov Y, Sanders KM, Ward SM. *Kit* signaling is essential for development and maintenance of interstitial cells of Cajal and electrical rhythmicity in the embryonic and gastrointestinal tract. *Dev Dyn* 236: 60−72, 2007

Cayabyab FS, DeBruin H, Jimenez M, Daniel EE. Ca^{2+} role in myogenic and neurogenic activities of canine ileum circular muscle. *Am J Physiol* 271: G1053−G1066, 1996

Dickens EJ, Edward FR, Hirst GDS. Selective knockout of intramuscular interstitial cell reveals their role in the generation of slow waves in mouse stomach. *J Physiol* 531: 827−833, 2001

Goto K, Matsuoka S, Noma A. Two types of spontaneous depolarizations in the interstitial cells freshly prepared from the murine small intestine. *J Physiol* 559: 409−420, 2004

Dickens EJ, Hirst GDS, Tomita T. Identification of rhythmically active cells in guinea-pig stomach. *J Physiol* 514: 515−531, 1999

Hamil OP, Marty A, Neher E, Sakamnn B, Sigworth FJ. Improved patch-clamp technique for high resolution current from cells ands cell-free membrane patches. *Pflügers Arch* 391: 85−100, 1981

Hennig GW, Hirst GD, Park KJ, Smith CB, Sanders KM, Ward SM, Smith TK. Propagation of pacemaker activity in the guinea-pig antrum. *J Physiol* 556: 585−599, 2004

Hirst GD, Edward FR. Generation of slow waves in the antral region of guinea-pig stomach - a stochastic process. *J Physiol* 535:

165−180, 2001
Hirst GDS, Ward SM. Interstitial cells: involvement in rhythmicity and neural control of gut smooth muscle. *J Physiol* 550: 337−346, 2003
Huizinga JD, Thuneberg L, Kluppel M, Malysz J, Mikkelsen HB, Bernstein A. *W/Kit* gene required for interstitial cells of Cajal and for intestinal pacemaker activity. *Nature* 373: 347−349, 1995
Kim YC, Koh SD, Sanders KM. Voltage-dependent inward currents of interstitial cells of Cajal from murine colon and small intestine. *J Physiol* 541: 797−810, 2002
Kito Y, Suzuki H. Pacemaker frequency is increased by sodium nitroprusside in the guinea pig gastric antrum. *J Physiol* 546: 191−205, 2003
Kito Y, Ward SM, Sanders KM. Pacemaker potential generated by interstitial cells of Cajal in the murine intestine. *J Physiol* 288: C710−C720, 2005
Klüppel M, Huizinga JD, Malysz J, Bernstein A. Developmental origin and Kit- dependent development of the interstitial cells of Cajal in the mammalian small intestine. *Dev Dyn* 211: 60−71, 1998
Koh SD, Jun JY, Kim TW, Sanders KM. A Ca^{2+}-inhibited non-selective cation conductance contributes to pacemaker currents in mouse interstitial cells of Cajal. *J Physiol* 540: 803−814, 2002
Koh SD, Monaghhan K, RoS, Mason HS, Kenyon JL, Sanders KM. Novel voltage-dependent non-selective cation conductance in murine colonic myocytes. *J Physiol* 533: 341-355, 2001
Koh SD, Sanders KM, Ward SM. Spontaneous electrical rhythmicity in cultured interstitial cells of Cajal from the murine small intestine. *J Physiol* 513: 203−213, 1998
Komuro T, Tokui K, Zhou DS. Identification of interstitial cells of Cajal. *Histol Histopathol* 11: 769−786, 1996
Kubota M, Kanda E, Ida K, Sakakihara Y, Hayashi M. Severe gastrointestinal dysmotility in a patient with congenital myopathy: causal relationship to decrease of interstitial cells of Cajal. *Brain Develop* 27: 447−450, 2005
Lammers WJ, Stephen B, Adeghate E, Ponery S, Pozzan O. The slow wave does not propagate across the gastroduodenal junction in the isolated feline preparation. *Neurogastroenterol Motil* 10: 339−349, 1998
Langton P, Ward SM, Carl A, Norell MA, Sanders KM. Spontaneous electrical activity of interstitial cells of Cajal isolated from canine proximal colon. *Proc Natl Acad Sci* 86: 7280−7284, 1989
Lee HK, Sanders KM. Comparision of ionic currents from interstitial cells and smooth muscle cells of canine colon. *J Physiol* 460: 135−152, 1993
Lee JI, Park HJ, Kamm MA, Talbot IC. Decreased density of interstitial cells of Cajal and neuronal cells in patients with slow-transit constipation and acquired megacolon. *J Gastroenterol Hepatol* 20: 1292−1298, 2005
Malysz J, Richaedson D, Farraway L, Christen MOM, Huizinga JD. Generaion of slow wave type action potentials in the mouse small intestine involves a non-L-type calsium channel. *Can J Physiol Pharmacol* 73: 1502−1511, 1995
Ördög T, Redelman D, Miller LJ, Horváth VJ, Zhong Q, Almeida-Porada G, Zanjani ED, Horowitz B, Sanders KM. Purification of interstitial cells of Cajal by fluorescence-activated cell sorting. *Am J Physiol* 286: C448−C456, 2004
Oue T, Puri P. Smooth muscle cell hypertrophy versus hyperplasia in infantile hypertrophic pyloric stenosis. *Pediatric Res* 45: 853−857, 1999
Pucovsky V, Moss Ray, Bolton TB. Non-contractile cells with thin processes resembling interstitial cells of Cajal found in the wall of guinea-pig mesenteric arteries. *J Physiol* 552: 119−133, 2003
Sanders KM. A case for interstitial cells of Cajal as pacemakers and mediators of neurotransmission in the gastrointestinal tract. *Gastroenterology* 111: 492−515, 1996
Sergeant GP, Hollywood MA, McCloskey KD, Thornbury KD, McHale NG. Specialized pacemaking cells in the rabbit urethra. *J Physiol* 526: 359−366, 2000
Thomsen L, Robinson TL, Lee JCF, Farraway LA, Hughes MJG, Andrew DW, Huizinga JD. Interstitial cells of Cajal generate a rhythmic pacemaker current. *Nat Med* 4: 848−851, 1998
Torihashi S, Ward SM, Nishikawa S, Kobayashi S, Sanders KM. c-*Kit*-dependent development of interstitial cells and electrical activity in the murine gastrointestinal tract. *Cell Tissue Res* 280: 97−111, 1995
Torihashi S, Ward SM, Sanders KM. Development of c-*Kit*-positive cells and the onset of electrical rhythmicity in murine small intestine. *Gastroenterology* 112: 144−155, 1997
Wang B, Kunze WA, Zhu Y, Huizinga JD. In situ recording from gut pacemaker cells. *Pflügers Arch* 457: 243−251, 2008
Wang XY, Lammers WJEP, Bercik P, Huizinga JD. Lack of pyloric interstitial cells of Cajal explains distinct peristalsis motor patterns in stomach and small intestine. *Am J Physiol* 289: G539−G549, 2005
Wang XY, Paterson C, Huizinga JD. Cholineregic and nitrergic innervation of ICC-DMP and ICC-IM in the human small intestine. *Neurogastroenterol Motil* 15: 531−543, 2003
Ward SM, Burns AJ, Torihashi S, Sanders KM. Mutation of the proto-oncogene c-*Kit* blocks development of interstitial cells and electrical rhythmicity in murine intestine. *J Physiol* 480: 91−97, 1994
Ward SM, Dixon RE, Faoite A, Sanders KM. Voltage-dependent calcium entry underlies propagation of slow waves in canine gastric antrum. *J Physiol* 561: 793−810, 2004
Ward SM, Sanders KM. Upstroke potential of electrical slow waves in canine colonic smooth muscle due to nifedipine-resistant calcium current. *J Physiol* 455: 321−337, 1992
Xu WX, Kim SJ, Kim SJ, So I, Kang TM, Rhee JC, Kim KW. Effect of stretch on calcium channel currents recorded from the antral myocytes of guinea-pig stomach. *Pflügers Arch* 432: 159−164, 1996